Identification of Critical Residues in Novel Drug Metabolizing Mutants of Cytochrome P450 BM3 Using Random Mutagenesis

Barbara M. A. van Vugt-Lussenburg, Eva Stjernschantz, Jeroen Lastdrager, Chris Oostenbrink, Nico P. E. Vermeulen,* and Jan N. M. Commandeur

LACDR/ Division of Molecular Toxicology, Department of Pharmacochemistry, Vrije Universiteit, De Boelelaan 1083, 1081 HV Amsterdam, The Netherlands

Received July 28, 2006

Previously, we've described a site-directed triple mutant of cytochrome P450 BM3 (BM3) that is able to convert various drugs (van Vugt-Lussenburg, B. M. A., et al. *Biochem. Biophys. Res. Commun.* **2006**, *346*, 810−818). In the present study, random mutagenesis was used to improve the activity of this mutant. With three generations of error-prone PCR, mutants were obtained with 200-fold increased turnover toward drug substrates dextromethorphan and 3,4-methylenedioxymethylamphetamine. The initial activities of these mutants were up to 90-fold higher than that of human P450 2D6. These highly active drug metabolizing enzymes have great potential for biotechnology. Using sequencing analysis, the mutations responsible for the increase in activity were determined. The mutations that had the greatest effects on the activity were F81I, E267V, and particularly L86I, which is not located in the active site. Computer modeling studies were used to rationalize the effects of the mutations. This study shows that random mutagenesis can be used to identify novel critical residues, and to increase our insight into P450s.

Introduction

Cytochromes P450 (P450s[a]) are involved in the metabolism of most drugs currently on the market.[2] Because of their broad substrate range and catalytic diversity, there is an increasing interest to use P450s in biotechnology, for example for the production of pharmaceuticals or the optimization of lead compounds and existing drugs.[3,4] Some disadvantages of the use of the membrane-bound human drug-metabolizing P450s are their low expression levels and stability, the requirement of a redox partner, and their generally low catalytic activities.[5,6] The soluble P450 BM3 (BM3) from *Bacillus megaterium*[7] would be a good candidate for use as a biocatalyst in the pharmaceutical industry. In BM3, the reductase domain is fused to its catalytic heme domain, so no coexpression of a separate redox partner is required. Furthermore, this enzyme has the highest catalytic activity ever recorded for a P450, is easily overexpressed in *E. coli*, and has a high stability.[5] Although the natural substrates of BM3 are fatty acids, it can be easily manipulated by mutagenesis to obtain enzymes that are able to convert a wide variety of non-natural substrates such as indol, alkanes, and propranolol.[8−10] Recently, we described a site-directed triple mutant of BM3, R47L/F87V/L188Q, that is able to convert various drug-like compounds.[1] The catalytic activity of this mutant, however, was still up to 125-fold lower than that of human P450s. In the present study we used random mutagenesis to improve the catalytic activity of the triple mutant. Libraries of random mutants were generated using error-prone PCR, and mutants with improved activity were selected using a whole-cell fluorescent screening assay with various alkoxyresorufins.[11] In addition, an LC-MS based whole-cell screening assay to measure dextromethorphan metabolism was developed. Computer modeling studies were used to rationalize the strongly increased enzyme activities observed with some of the obtained mutants.

Results

Selection of Random Mutants of BM3. As a template for random mutagenesis, the triple mutant BM3 R47L/F87V/L188Q was used. After the first round of mutagenesis, 400 colonies were screened. The benzyloxyresorufin-O-dealkylation (BROD) activities were plotted against the pentoxyresorufin-O-dealkylation (PROD) and methoxy/ ethoxyresorufin-O-dealkylation (MROD/EROD) activities in a scatter plot, in order to visualize the range of activities and the variation in substrate selectivity of the random mutants (Figure 1A and 1B). Compared to the triple mutant controls, mutant M01 showed no increased BROD activity, and a decreased PROD activity, but a significantly higher MROD/EROD activity. The triple mutant and most other mutants did not show any MROD/EROD activity in the screening procedure (Figure 1B). Mutant M02 showed a higher activity toward all substrates. Mutants M03 and M04 both showed increased BROD activity.

In a second round, M01 and M02 were selected as a template for further mutagenesis, based on their increased MROD/EROD activity (M01 and M02) and PROD activity (M02) (Figure 1A and 1B). To be able to screen for mutants with improved activity toward dextromethorphan, an LC-MS screening assay was used. To improve the permeability of the cells, the known permeabilizing agents Triton X-100 and EDTA were added to the assay. The presence of 10 or 25 mM EDTA did not increase the amount of product formed, but with 0.1% Triton X-100, product formation was 2.5-fold higher than in the absence of permeabilizing agent (data not shown). The mutants originating from error-prone PCR on M01 and M02 were screened both with the alkoxyresorufin screening assay and the dextromethorphan screening assay. With M01 as template, 350 colonies were screened, resulting in the identification of mutant M05, that had a 6-fold increased BROD activity and PROD activity (Figure

* Corresponding author. Tel.: +31-20-5987595; Fax: +31-20-5987610. E-mail: npe.vermeulen@few.vu.nl.

[a] Abbreviations: P450, cytochrome P450; BM3, P450 BM3; BROD, benzyloxyresorufin O-dealkylation; PROD, pentoxyresorufin O-dealkylation; EROD, ethoxyresorufin O-dealkylation; MROD, methoxyresorufin O-dealkylation; MDMA, 3,4-methylenedioxymethylamphetamine; MDA, 3,4-methylenedioxyamphetamine; 3-MM, 3-methoxymorphinan; AU, arbitrary units.

10.1021/jm0609061 CCC: $37.00
Published on Web 01/18/2007

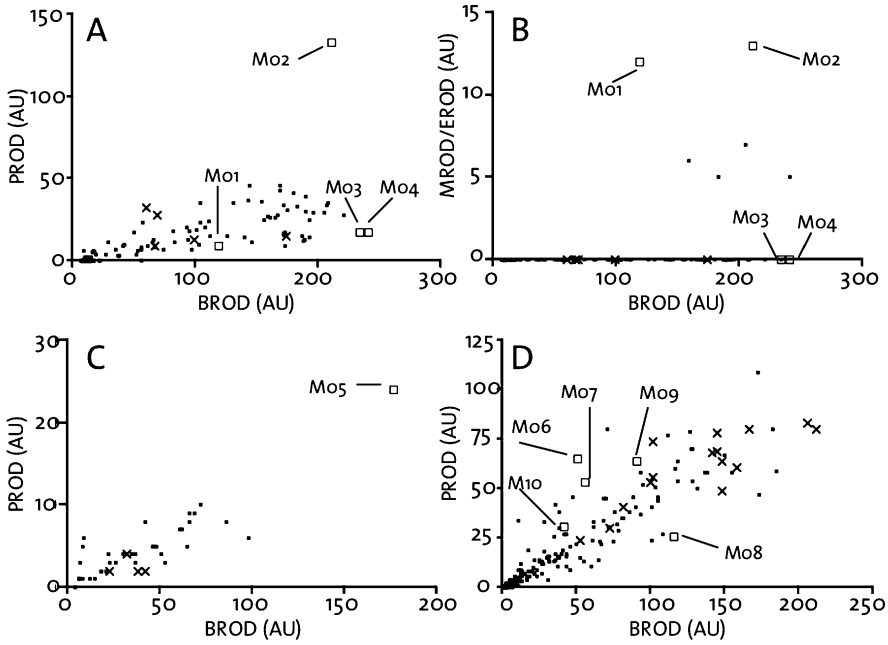

Figure 1. Screening assays with alkoxyresorufins. Random mutants in PROD vs BROD scatter plots (A, C, D) or MROD/EROD vs BROD scatter plots (B). A and B: First generation mutants with BM3 R47L/F87V/L188Q as mutagenesis template. C: second generation mutants with M01 as mutagenesis template. D: second generation mutants with M02 as mutagenesis template. Data were obtained from 96-well plate screening assays. Each dot represents one mutant. Mutants that showed no activity have not been included. '×' represents nonmutated controls (A/ B: triple mutant. C: M01. D: M02). Open squares represent mutants that have been selected for further investigation.

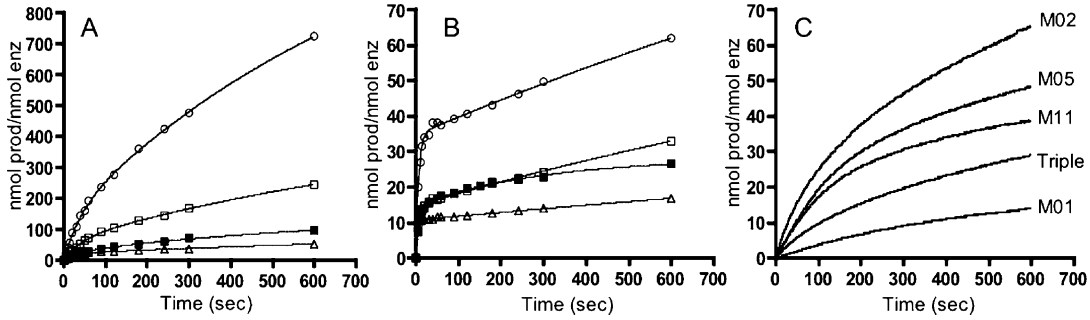

Figure 2. Time dependence of the enzyme activity. Time dependence of dextromethorphan (A) and MDMA (B) N-demethylation, and benzyloxyresorufin O-dealkylation (C), by mutants M11 (open circles), M05 (open squares), M01 (closed squares), and M02 (open triangles). For benzyloxyresorufin, the activity of the triple mutant was also measured. Product formation from dextromethorphan and MDMA by the triple mutant was too low to be detected accurately under the conditions used. Curves were fitted to the following equation, derived from refs 12, 33. product $= [P_1(1 - e^{-P2t})]/P_2 + P_3t$.

1C) and 3.7-fold increased dextromethorphan demethylation activity compared to M01. 600 Colonies were screened that had M02 as a starting point. On the basis of the BROD/PROD scatter plot, five mutants were selected for further studies (colonies M06, M07, M08, M09, and M10, Figure 1D).

In a third round of error-prone PCR, M05 was used as a template, and only the dextromethorphan screening assay was used. Fifty colonies were screened, and mutant M11 with 1.5-fold improved activity was selected for further characterization (data not shown).

Characterization of the Random Mutants. MDMA was metabolized into three metabolites by all the random mutants tested. The main metabolite was 3,4-methylenedioxyamphetamine (MDA), the second most abundant metabolite was *N*-hydroxy-3,4-methylenedioxymethylamphetamine, and the minor metabolite was 3,4-dihydroxymethylamphetamine. This metabolic profile was also observed for the triple mutant in a previous study.[1] Dextromethorphan was N-demethylated to 3-methoxymorphinan (3-MM) by all mutants. Additionally, with LC-MS, trace amounts of two mono-hydroxylated metabolites were observed for M02 that could not be detected with fluorescence detection. In this study, data is presented only for the major metabolites MDA and 3-MM. Some of the mutants that were selected from the screening assays did not show increased metabolism toward the substrates tested. These mutants, M03, M04, and M06−M10, were therefore not investigated further. The mutants further analyzed in this study are M01, M02, M05, and M11.

Analysis of the time dependence of the enzyme activity of the random mutants showed that these enzymes all have a very high initial activity during the first 50 s of the reaction, followed by decrease to a slower rate of metabolism (Figure 2) which was linear for at least 60 min (data not shown). Product formation by the triple mutant was too low to be determined accurately in the first 10 min of the reaction. To study the initial enzyme activity in more detail, stopped-flow experiments were performed with the four random mutants and the triple mutant using the substrate benzyloxyresorufin. This setup allowed a much higher sampling frequency (10 s^{-1}), resulting in more accurate data. Because benzyloxyresorufin is a better substrate for the triple mutant than dextromethorphan and MDMA, the time course of this mutant could also be studied using this setup.

Table 1. Initial, Fast Enzyme Rates and Slow Enzyme Rates As Determined from the Product Formation/Time Curves in Figure 2[a]

	triple mutant	mutant M01	mutant M02	mutant M05	mutant M11	hP450 2D6[F120A][c]
Dex P_1	nd[b]	41.8	47.7	91.2	212.9	4.5 ± 0.3[13]
Dex P_2	nd[b]	1.2	2.0	1.1	1.0	
Dex P_3	nd[b]	6.2	3.0	16.4	51.0	
MDMA P_1	nd[b]	97.8	216.8	158.9	313.9	3.5 ± 0.1[32]
MDMA P_2	nd[b]	5.7	20.4	10.5	8.9	
MDMA P_3	nd[b]	1.0	0.6	1.8	2.7	
BROD P_1	6.1	2.3	18.5	13.9	13.3	
BROD P_2	0.5	0.2	0.6	0.4	0.5	
BROD P_3	1.7	0.3	3.7	1.8	1.3	

[a] Data was obtained for dextromethorphan (Dex) and 3,4-methylenedioxy-methylamphetamine (MDMA) N-demethylation, and for benzyloxyresorufin O-dealkylation (BROD). Values were obtained by fitting the curves to the following equation, derived from:[12,33] product $= [P_1(1 - e^{-P2t})]/P_2 + P_3t$.[34] The first derivative of this equation, $P_1(e^{-P2t}) + P_3$, shows that this term describes an initial 'fast' rate (P_1) followed by a deactivation process (exponential rate: P_2) to a 'slow' rate (P_3). P_1 and P_3 are in nmol product/min/nmol enzyme, and P_2 is in min^{-1}. [b] For the triple mutant, product formation from dextromethorphan and MDMA was too low to be detected accurately under the conditions used (nd). [c] For comparison, literature V_{max} values for hP4502D6[F120A] are included (for dextromethorphan: O-demethylation. For MDMA: N-demethylation).

As was observed for dextromethorphan and MDMA, the stopped-flow data showed a high initial activity followed by a slower phase. The rates for the slow phase, the exponential decay, and the fast phase have been estimated by fitting the data in Figure 2 to the empirical function used previously by Noble et al.[12] Results are given in Table 1. For comparison, the rates of metabolism for the human P450 2D6 mutant 2D6-[F120A] are also given. P450 2D6[F120A] is chosen for comparison rather than wild-type P450 2D6, because 2D6-[F120A] is also able to form MDA at appreciable rates, while wild-type P450 2D6 forms mainly 3,4-dihydroxymethylamphetamine. The dextromethorphan O-demethylation activities are very similar for wild-type 2D6 and 2D6[F120A].[13] At a substrate concentration of 2 mM, the initial reaction rate of dextromethorphan N-demethylation by the BM3 random mutants was up to 47-fold higher than the V_{max} of dextromethorphan O-demethylation by P450 2D6[F120A], and the slow rates were up to 11-fold higher (Table 1). At a substrate concentration of 3 mM, the initial rate of MDA formation by the BM3 mutants was 30 to 90-fold higher than the V_{max} of P450 2D6[F120A], and the slow rates were similar to the V_{max} of P450 2D6[F120A] (Table 1).

For dextromethorphan and benzyloxyresorufin metabolism, the difference between the slow phase and the fast phase is approximately 4 to 15-fold, while for MDMA metabolism this difference is 100 to 360-fold (Table 1). The rate of inactivation, P_2, is similar for dextromethorphan and BROD, but for MDMA, P_2 is up to 30-fold higher. Further studies are required to elucidate the mechanisms underlying this substrate-dependent biphasic behavior.

To study the substrate concentration dependence of the reaction, product formation was plotted against substrate concentration (Figure 3). Because of the nonlinear time course described above, no enzyme kinetic parameters were assessed.

For dextromethorphan metabolism, mutant M11 showed the highest activity (Figure 3A). Product formation by M11 after 20 min at 2 mM substrate concentration was 200-fold higher than by the triple mutant. Mutant M01 and M02 metabolized dextromethorphan with 20 to 25-fold higher turnover compared to the triple mutant, and the evolution from M01 to M05 resulted in a further 3-fold improvement. Evolution from M05 to M11 increased the activity another 2.5-fold.

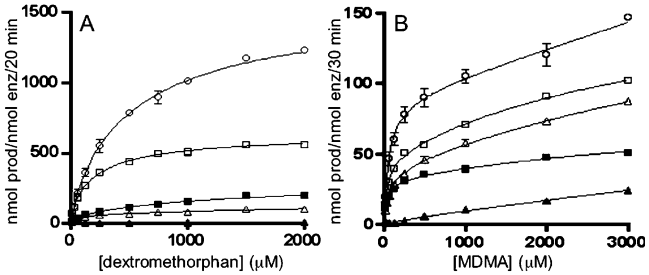

Figure 3. Substrate concentration dependence of dextromethorphan and MDMA N-demethylation. Product formation/[S] curves for dextromethorphan (A) and MDMA (B) N-demethylation by mutants M11 (open circles), M05 (open squares), M01 (closed squares), M02 (open triangles), and the triple mutant (closed triangles).

For MDMA metabolism, M11 again showed the highest activity, 5-fold higher than the triple mutant at 3 mM substrate concentration (Figure 3B). Product formation by M02 after 30 min was 4-fold higher than by the triple mutant, and by M01 it was 2-fold higher than the triple mutant. Evolution from M01 to M05 resulted in a 2-fold increase in activity, and for M11, product formation was another 1.5-fold higher.

Mutagenesis Results and Interpretations from Modeling. The mutations present in M01, M02, M05, and M11 were identified using DNA sequencing (Table 2). Computer modeling of the mutants was used to suggest explanations for the experimental results. From the models of the mutants it could clearly be seen that the F87V mutation, present in all mutants, seems to be responsible for making the catalytic site accessible to bulkier substrates by opening up the site directly above the heme-iron, as has been shown before by others.[14] R47 is positioned at the entrance of the suggested substrate access channel and has been described to be important for substrate recognition, forming interactions with and anchoring the negatively charged carboxylate group of the natural substrates.[9,12] The substrates considered in this study both display a positively charged amine. The R47L mutation is thus expected to be favorable due to the removal of a positive charge in the entrance of the substrate access channel. L188 is also located in the entrance of the mainly hydrophobic access channel. Exchanging R47, which is one of the few polar side chains, with a leucine could lead to an unfavorably nonpolar environment in the access channel. Reintroducing a polar side chain with the L188Q mutation could reverse that effect.[14]

Mutant M01 had two additional mutations compared to the triple mutant: E267V and G415S. In the crystal structure, G415 is not in the proximity of the active site, whereas E267 is located in the active site on helix I (Figure 4). To establish the role of the E267V mutation in M01 experimentally, the mutation E267V was introduced into the triple mutant using site-directed mutagenesis. This resulted in mutant M01a (Table 2). In activity assays with dextromethorphan and MDMA, M01a behaved identical to M01 (data not shown), which suggests that the E267V mutation is solely responsible for the increased activity of M01.

In the substrate-free crystal structure (PDB ID 1BU7) the side-chain of E267 is positioned approximately 3 Å from the K440 side-chain and directed away from the active site facing the surface of the protein, interacting with K440. It forms part of the active site channel exit as described by Haines et al.[15] During simulation of the model of the E267V mutant, the side chain of V267 turns toward the active site, possibly closing off the active site channel exit and forming a hydrophobic pocket together with L181, that turns in toward V267 (Figure 5A). This

Table 2. Mutations Identified in the Random Mutants of BM3 Determined by DNA Sequencing

triple mutant	mutant M01	mutant M02	mutant M05	mutant M11	*mutant M01a*[b]	*mutant M02a*[b]	*mutant M02b*[b]
R47L	R47L	R47L	R47L	R47L E64G	*R47L*	*R47L*	*R47L*
			F81I	F81I			
		L86I				*L86I*	
F87V	F87V	F87V	F87V	F87V E143G	*F87V*	*F87V*	*F87V*
L188Q	L188Q E267V	L188Q	L188Q E267V	L188Q E267V	*L188Q* *E267V*	*L188Q*	*L188Q*
	(G415S)[a]	(N319T)[a]	(G415S)[a]	(G415S)[a]			*(N319T)*[a]

[a] The mutations in parentheses have been shown not to contribute to the enhanced activities of the mutants. [b] The mutants M01a, M02a, and M02b, in *italic*, are site-directed mutants.

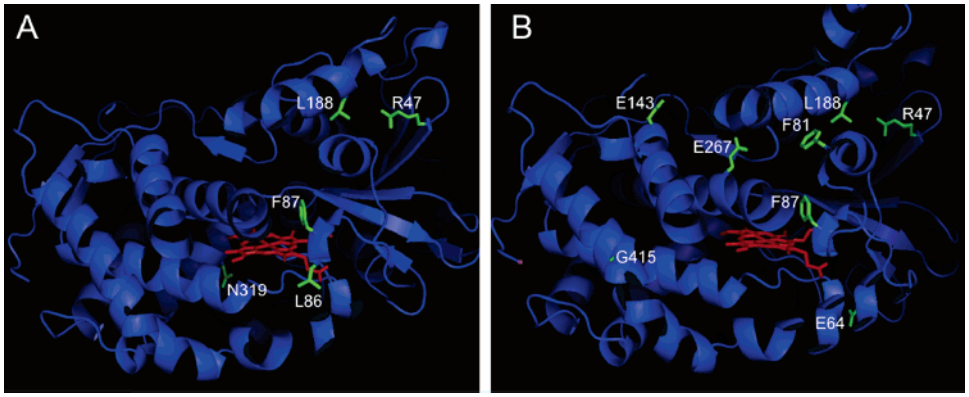

Figure 4. Crystal structure of the active site of BM3 (PDB ID 1BU7). The heme group is shown in red. The residues that were altered in mutant M02 (A) and M11 (B) are labeled by their amino acid numbers and depicted in green in stick format.

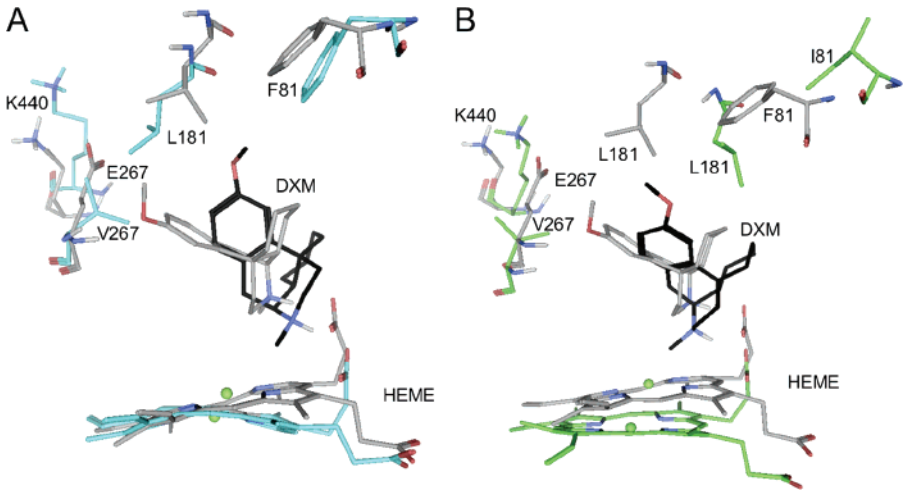

Figure 5. View of dextromethorphan in the superposed active sites of the triple mutant and mutant M01 (A) or M05 (B) after 1 ns of simulation. The carbon atoms of the triple mutant are colored gray (A and B). The M01 protein carbon atoms are colored cyan (A), and the M05 protein carbon atoms are colored green (B). Dextromethorphan (DXM) is depicted in gray in the triple mutant, and in black in mutant M01 and M05. The side chain of E267 of the triple mutant is directed out from the active site, interacting with K440, whereas V267 of M01 is directed in toward the active site, possibly closing off the active site channel exit and forming a hydrophobic pocket together with L181, that turns in toward V267. In the M05 mutant the backbone of I81, situated in the B′ helix, is shifted to the right in the figure. This allows for a shift of the backbone around L181, situated in the F helix. The Cα's of the two L181 residues are approximately 3 Å apart in this comparison.

may tighten the interactions in the hydrophobic substrate pocket or allow for substrate orientations that are more favorable for metabolism.

In mutant M05, which originated from M01, one additional mutation was found: F81I. F81 is located on the B′ helix with its side-chain directed toward the interior of the protein but not directly in the active site (Figure 4B). Preliminary data from molecular dynamics simulations suggest that in the F81I mutant the side chain of I81 shifts slightly, which as a result induces a large conformational changes of L181. This conformational change affects the shape of the hydrophobic substrate pocket (Figure 5B). This could also influence the orientation of the ligand in the active site and thus affect the rate of metabolism.

Mutant M11, originating from M05, had the two additional mutations E64G and E143G. Both mutations are located on the surface of the P450 domain (Figure 4). In the crystal structure of BM3, E64 is located at the interface of the heme domain and the FMN domain (PDB code 1BVY[16]). It remains to be investigated whether both mutations are required for the increased activity of M11. Because of their position on the

protein surface, they could be involved in substrate entrance or product exit, or in interaction with the reductase domain and the electron transport chain.

In M02, which had the triple mutant as template, two additional mutations were found: L86I and N319T. L86 is not located in the active site but in close vicinity of one of the propionate side-chains of the heme porphyrin (Figure 4A). The localization of this residue makes it unlikely to be directly involved in substrate binding. Residue N319 is more distant from the substrate binding site and heme than L86 (Figure 4A). To establish the roles of the L86I and N319T mutations experimentally, both mutations were introduced into the triple mutant separately using site-directed mutagenesis. This resulted in mutants M02a and M02b (Table 2). Enzyme activity assays with dextromethorphan and MDMA showed that M02b has the same activity as the triple mutant, while M02a has the same activity as mutant M02 (data not shown). This shows that the mutation N319T does not play a significant role. The increased activity of M02 is therefore caused by the rather conservative L86I mutation. Molecular dynamics simulations showed that this conservative substitution results in conformational changes in the surrounding residues, but the implications of these changes requires more detailed studies.

Discussion

We recently described a site-directed triple mutant of BM3 that is able to metabolize drugs.[1] The aim of the current study was to further increase the activity of this mutant by random mutagenesis, since it was still low compared to several human drug-metabolizing P450s. In three generations of random mutagenesis using error-prone PCR, in total 1400 colonies were picked and screened. Four mutants with a strongly increased activity toward dextromethorphan and MDMA were identified. The largest improvements were observed for dextromethorphan, where the product formation was increased up to 200-fold when compared to the triple mutant. The initial activities of the random BM3 mutants were up to 90-fold higher than of P450 2D6 (Table 1). So far, random mutagenesis studies on mammalian P450s have shown that even after several cycles of mutagenesis, the increase in activity rarely exceeds a factor 10.[17]

When the incubation with BM3 M11 would be upscaled to 1 L of batch culture (~500 nmol P450), approximately 200 mg of 3-MM can be produced in 20 min. For comparison, the only other BM3 mutant described that metabolizes drugs, BM3 9C1, can produce 70 mg propranolol metabolites per liter of culture in 180 min.[10] The biotransformation reactions that are currently used in the pharmaceutical industry have a volumetric productivity ranging from 0.2 mg/L to 14 g/L.[18]

BM3 is one of the most intensively studied P450s, and it has been subjected to several random- and site-directed mutagenesis studies. In this study, several unique mutations that have a big effect on the catalytic activity of BM3 were identified that have not been investigated before. The most striking effects were observed for the mutations L86I in mutant M02, and E267V in mutant M01.

It is very surprising that a conservative substitution like L86I can have such dramatic effects on the catalytic activity. Interestingly, a reverse mutation, I115L, was previously found to produce the opposite effect in insect P450 6B1.[19] Sequence alignment of P450 6B1 and BM3 revealed that I115 and L86 are located at the same position. It was suggested that residue I115 is positioned along the path of a product exit channel.[19] The conservative mutation I115L is suggested to block this channel, significantly limiting the catalytic capacity of P450 6B1. Accordingly, one hypothesis is that in BM3 the L86I mutation opens up a product exit channel, which increases the catalytic efficiency of the enzyme. L86 and I115 are positioned directly next to the heme (Figure 4); other possibilities are that the I115L and L86I mutations influence the heme group, or electron transport.[19] Molecular dynamics simulations showed that for L86I, the small change in the amino acid side chain has a pronounced effect on the conformation of the surroundings. Whether this conformational change results in the opening of a substrate channel, or rather influences the position of the heme in the protein or the electron transport chain, requires more detailed studies.

It has been reported that a mutant of BM3 where the acidic E267 was converted into a glutamine (E267Q) had up to 280-fold decreased activity for several fatty acids.[20] In the present study, on the contrary, the mutation E267V resulted in a 25-fold increased catalytic activity toward dextromethorphan compared to the triple mutant. Molecular dynamics simulations have shown that the E267V mutation results in a conformational change in the hydrophobic substrate pocket, which could affect the orientation of the ligand and thus the catalytic activity.

Time-dependent inactivation of BM3 was observed previously for lauric acid metabolism by the mutants F87G and F87Y.[12] It was hypothesized that during turnover, these mutants undergo an irreversible conformational change that results in decreased activity. Also in other enzymes, this phenomenon called 'rapid burst kinetics' has been observed.[21] In the present study, all mutants tested also showed this nonlinear behavior (Figure 2). After a fast initial activity the enzyme activities decayed to a much slower linear phase. Interestingly, the inactivation rate for MDMA metabolism appeared to be 10-fold higher than for dextromethorphan metabolism, and 30-fold higher than for BROD. If it would be possible to prevent this inactivation, the catalytic efficiency of the enzymes would increase another 4- to 360-fold (Table 1).

Conclusions

The mutants described in this study could be used as a starting point for further random or site-directed mutagenesis, to further increase their activity or to further broaden their substrate specificity or alter their metabolic profile. For drug discovery, mutants with a broad metabolic profile would be most useful, while for the biosynthesis of specific drugs or drug metabolites, mutants with a high degree of regiospecificity are required. The combination of random mutagenesis and molecular modeling can yield novel insights in the mechanism of P450s. Small changes in amino acids can unexpectedly have dramatic effects on the activity, as seen in the present study for the conservative mutation L86I.

Materials and Methods

Random Mutagenesis. The triple mutant of BM3 was constructed in the plasmid pT1-P450BM3 and transformed into *E. coli* DH5α cells as described earlier.[11] Libraries of random mutants were constructed using error-prone PCR. To enable cloning of the heme domain, a *SacI* restriction site was constructed 130 bp upstream of C-terminus of the heme domain by introducing a silent mutation in residue L431, as described in ref 22. The PCR was carried out in a 50 μL reaction mixture containing template plasmid (5 ng), forward primer (5′-cacaggaacc*ggatcc*catgacaattaaagaa-3′, N-terminal *BamHI* site underlined) and reverse primer (5′-gtgaaggaataccgccaa-3′) (20 pmol each), dATP and dGTP (0.2 mM each), dCTP and dTTP (1 mM each), $MgCl_2$ (7 mM), 10x *Taq* polymerase buffer (5 μL), and *Taq* polymerase (5 units). The PCR was performed in a thermocycler for 30 cycles (95 °C, 45 s; 50 °C, 30 s; 72 °C, 60 s).

The PCR product was digested with *BamHI* and *SacI* and ligated into the pT1 expression vector digested with the same restriction enzymes. The resulting plasmid was transformed into lipopolysaccharide defective (LPS^d) *E. coli* DH5α cells as described previously.[11]

The QuikChange Site-Directed mutagenesis kit (Stratagene) was used to introduce the mutations L86I, E267V, and N319T into the triple mutant R47L/ F87V/L188Q. Sequences of the forward primers, with the altered residues underlined, were as follows: L86I gcaggagacggg*ata*gtaacaagctggacg; E267V taattgcgggacac*gta*acaacaagtggt; N319T atgtcggcatggtctta*acc*gaagcgctgc. The reverse primers used were the exact complements of the forward primers. DNA sequencing was performed to confirm the presence of the desired mutations.

Expression of BM3 Mutants. Colonies with random mutants of BM3 were picked from agar plates and transferred to 96-well plates containing 200 μL/well of LB medium supplemented with 50 μg/mL ampicillin. As a control, four wells were inoculated with cells containing the plasmid with the nonmutated parent DNA. Cells were grown overnight at 37 °C and 650 rpm in a well plate shaking incubator (Denley Vortemp, Thermo Electron). After overnight growth, 20 μL of cell suspension was transferred to a 96-well plate containing 180 μL/well TB medium (24 g/L yeast extract, 12 g/L tryptone, 4 mL/L glycerol) with additives (1 mM δ-aminolevulinic acid, 400 μL/L trace elements,[23] 0.5 mM thiamine, 50 μg/mL ampicillin). Cells were grown for 3 h at 37 °C and 650 rpm before expression was induced by increasing the temperature to 40 °C. Expression was allowed to continue for approximately 5 h before the cells were harvested. The plates were centrifuged (3000*g*, 15 min, 4 °C), and the medium was discarded. Cell pellets were stored at −20 °C until use.

Screening on Alkoxyresorufin O-Dealkylation Activity. The 96-well plates with cells were thawed and resuspended in 200 μL/well cold 100 mM potassium phosphate (KPi) buffer, pH 7.4, and 20 μL of cell suspension was transferred to three black 96-well plates containing 160 μL/well 100 mM KPi buffer pH 7.4 with 12.5 μM substrate (benzyloxyresorufin, pentoxyresorufin, or a mixture of methoxy- and ethoxyresorufin). The reaction was initiated by the addition of 20 μL of an NADPH regenerating system resulting in final concentrations of 0.2 mM NADPH, 0.3 mM glucose-6-phosphate, and 0.4 units/mL glucose-6-phosphate dehydrogenase. Formation of the fluorescent product resorufin was monitored for 15 min at 24 °C on a Victor^2 1420 multilabel counter (Wallac, λ_{ex} = 530 nm, λ_{em} = 580 nm). Mutants with increased activity and/or altered selectivity toward different alkoxyresorufins compared to the nonmutated parent enzyme were cultured on a 300 mL scale as described previously[11] and were subsequently characterized using dextromethorphan and 3,4-methylenedioxymethylamphetamine (MDMA) as substrates.

Screening on Dextromethorphan N-Demethylation Activity. To identify BM3 mutants that can convert drugs with high activity, a high throughput screening assay was developed for dextromethorphan metabolism. For this assay, the 96-well plates with frozen cell pellets were thawed and resuspended in 180 μL/well cold 100 mM potassium phosphate (KPi) buffer, pH 7.4, containing 1 mM dextromethorphan and 0.1% Triton X-100. The reaction was initiated by the addition of 20 μL of an NADPH regenerating system as described above. The reaction was allowed to proceed for 3 h at 24 °C and was terminated by the addition of 20 μL of a 10% (v/v) $HClO_4$ solution. The plates were centrifuged (3000*g*, 15 min, 4 °C), and the supernatant was analyzed by LC-MS. LC separation was carried out using a C18 column (Phenomenex Luna 5 μm, 150 × 4.6 mm). The mobile phase consisted of 80% acetonitrile with 0.1% formic acid, and the flow rate was 0.5 mL/ min. Every 3 min, 10 μL of a sample was injected. The MS system used was an LCQ Deca mass spectrometer (Thermo Finnigan). Atmospheric pressure chemical ionization (APCI) was used, with a vaporizer temperature of 450 °C, N_2 as sheath gas (40 psi) and auxiliary gas (10 psi), and a needle voltage of 6000 V, and the heated capillary was 150 °C. The system was used in scan-mode, and the intensities of the MS signal at *m*/*z* 258 (demethylated dextromethorphan) of the mutants were compared to those of the nonmutated parent enzymes, and mutants with improved activity were cultured and characterized using dextromethorphan and MDMA as substrates.

Characterization of BM3 Mutants Using Dextromethorphan and MDMA. First, the linearity of product formation in time and the enzyme concentration dependence were determined. Incubations were performed for dextromethorphan and MDMA as described below, with a fixed substrate concentration of 250 μM, and various enzyme concentrations (25−200 nM), or with a fixed substrate concentration of 2 mM dextromethorphan or 3 mM MDMA and various incubation times (0−60 min). Based on these experiments (data not shown), the following conditions were chosen for further studies:

The dextromethorphan incubations were performed in 100 mM KPi buffer pH 7.4, with the *E. coli* cytosolic fraction containing 200 nM BM3 triple mutant or 100 nM of the random mutants. Substrate concentrations were used ranging from 0 to 4 mM (11 concentrations). The final volume of the incubations was 200 μL. The reactions were initiated by addition of 20 μL of an NADPH regenerating system as described above. The reaction was allowed to proceed for 20 min at 24 °C and terminated by the addition of 20 μL of a 10% (v/v) $HClO_4$ solution. Precipitated protein was removed by centrifugation (15 min, 4000*g*), and the supernatant was analyzed by HPLC. Metabolites were separated using a C18 column (Phenomenex Luna 5 μm, 150 × 4.6 mm) with a flow rate of 0.6 mL/min. The mobile phase consisted of 30% acetonitril with 0.1% triethylamine, set to pH 3.0 with $HClO_4$. Metabolites were detected with a fluorescence detector ($\lambda_{excitation}$ = 280 nm and $\lambda_{emission}$ = 311 nm) and also with LC-MS as described in ref 24. The dextromethorphan metabolite 3-methoxymorphinan (3-MM, N-demethylated dextromethorphan) was quantified using a standard curve of dextromethorphan, assuming that the fluorescence of dextromethorphan and 3-MM are comparable. Product formation was plotted against substrate concentration in GraphPad Prism 4.0.

For MDMA, incubations were performed as described for dextromethorphan. Substrate concentrations were used ranging from 0 to 3 mM (nine concentrations), and the incubation time was 30 min. The mobile phase consisted of 20% acetonitrile and 0.1% triethylamine, set to pH 3.0 using $HClO_4$. Metabolites were detected with a fluorescence detector ($\lambda_{excitation}$ = 280 nm and $\lambda_{emission}$ = 320 nm). Peak areas were determined using the Shimadzu Class VP 4.3 software package. The MDMA metabolite 3,4-methylenedioxyamphetamine (MDA) was quantified using a synthesized reference compound. Product formation was plotted against substrate concentration in GraphPad Prism 4.0.

Investigation of Nonlinear Behavior Using Stopped-Flow. To further investigate the observed nonlinear time course of product formation by some of the mutants, BROD activity was measured using a stopped-flow setup consisting of two syringes, a mixing chamber, and a cuvette (KinTek Corporation, Austin, TX). One syringe was filled with enzyme and substrate (enzymes: 10 nM final concentration; substrate: 10 μM final concentration). The second syringe was filled with an NADPH regenerating system as described. The system was at 24 °C. The reaction was initiated by mixing the contents of both syringes in a mixing chamber, immediately followed by a cuvette. The cuvette was positioned in a fluorometer ($\lambda_{excitation}$ = 530 nm and $\lambda_{emission}$ = 580 nm), and the reaction was monitored for 10 min. The sampling frequency was 10 s^{-1}. Data was plotted in GraphPad Prism 4.0.

Computer Modeling of the Random Mutants. The highly active mutants obtained were modeled based on the heme-binding domain, residues 1−455, of the substrate-free crystal structure, PDB code 1BU7.[16] The substrate-free structure was selected because the structure of the bulky, rigid substrate dextromethorphan strongly differs from the highly flexible palmitoyl-derivates present in the ligand-bound structures. Energy minimization of the mutant structures was performed using the MOE (Molecular Operating Environment) program.[25] Based on superimposition of the minimized mutant structures and the wild type structure, preliminary suggestions on the function and effect of the mutated residues could be made. Because the effects of the mutations on the activity were

much bigger for dextromethorphan than for MDMA, automated docking calculations were performed for dextromethorphan using GOLD.[26] To further study the effects of the mutations on the enzyme conformation, molecular dynamics simulations were performed on the resulting docked complexes using GROMOS05[27] and GROMACS,[28,29] using the GROMOS forcefield set 45A3.[30,31] The minimized protein−ligand complexes were centered in a periodic solvated box containing approximately 14 000 molecules. This system is gradually heated up to 300 K and equilibrated for 40 ps. Subsequently, 1 ns of free simulation was performed.

Acknowledgment. We gratefully acknowledge Dr. G. van der Zwan (Department of Analytical Chemistry and Applied Spectroscopy, Vrije Universiteit Amsterdam) for his advice and assistance in the modeling of the nonlinear time courses.

References

(1) van Vugt-Lussenburg, B. M. A.; Damsten, M. C.; Maasdijk, D. M.; Vermeulen, N. P. E.; Commandeur, J. N. M. Heterotropic and homotropic cooperativity by a drug-metabolising mutant of cytochrome P450 BM3. *Biochem. Biophys. Res. Commun.* **2006**, *346*, 810−818.

(2) Guengerich, F. P. Common and uncommon cytochrome P450 reactions related to metabolism and chemical toxicity. *Chem. Res. Toxicol.* **2001**, *14*, 611−650.

(3) Guengerich, F. P. Cytochrome P450 enzymes in the generation of commercial products. *Nat. Rev. Drug. Discovery* **2002**, *1*, 359−366.

(4) Urlacher, V. B.; Lutz-Wahl, S.; Schmid, R. D. Microbial P450 enzymes in biotechnology. *Appl. Microbiol. Biotechnol.* **2004**, *64*, 317−325.

(5) Munro, A. W.; Leys, D. G.; McLean, K. J.; Marshall, K. R.; Ost, T. W.; Daff, S.; Miles, C. S.; Chapman, S. K.; Lysek, D. A.; Moser, C. C.; Page, C. C.; Dutton, P. L. P450 BM3: the very model of a modern flavocytochrome. *Trends Biochem. Sci.* **2002**, *27*, 250−257.

(6) Urlacher, V.; Schmid, R. D. Biotransformations using prokaryotic P450 monooxygenases. *Curr. Opin. Biotechnol.* **2002**, *13*, 557−564.

(7) Narhi, L. O.; Fulco, A. J. Characterization of a catalytically self-sufficient 119,000-dalton cytochrome P-450 monooxygenase induced by barbiturates in Bacillus megaterium. *J. Biol. Chem.* **1986**, *261*, 7160−7169.

(8) Glieder, A.; Farinas, E. T.; Arnold, F. H. Laboratory evolution of a soluble, self-sufficient, highly active alkane hydroxylase. *Nat. Biotechnol.* **2002**, *20*, 1135−1139.

(9) Li, Q. S.; Schwaneberg, U.; Fischer, P.; Schmid, R. D. Directed evolution of the fatty-acid hydroxylase P450 BM-3 into an indole-hydroxylating catalyst. *Chemistry* **2000**, *6*, 1531−1536.

(10) Otey, C. R.; Bandara, G.; Lalonde, J.; Takahashi, K.; Arnold, F. H. Preparation of human metabolites of propranolol using laboratory-evolved bacterial cytochromes P450. *Biotechnol. Bioeng.* **2006**, *93*, 494−499.

(11) Lussenburg, B. M. A.; Babel, L. C.; Vermeulen, N. P. E.; Commandeur, J. N. M. Evaluation of alkoxyresorufins as fluorescent substrates for cytochrome P450 BM3 and site-directed mutants. *Anal. Biochem.* **2005**, *341*, 148−155.

(12) Noble, M. A.; Miles, C. S.; Chapman, S. K.; Lysek, D. A.; MacKay, A. C.; Reid, G. A.; Hanzlik, R. P.; Munro, A. W. Roles of key active-site residues in flavocytochrome P450 BM3. *Biochem. J.* **1999**, *339* (Pt 2), 371−379.

(13) Keizers, P. H. J.; Lussenburg, B. M. A.; de Graaf, C.; Mentink, L. M.; Vermeulen, N. P. E.; Commandeur, J. N. M. Influence of phenylalanine 120 on cytochrome P450 2D6 catalytic selectivity and regiospecificity: crucial role in 7-methoxy-4-(aminomethyl)-coumarin metabolism. *Biochem. Pharmacol.* **2004**, *68*, 2263−2271.

(14) Li, Q. S.; Ogawa, J.; Schmid, R. D.; Shimizu, S. Engineering cytochrome P450 BM-3 for oxidation of polycyclic aromatic hydrocarbons. *Appl. Environ. Microbiol.* **2001**, *67*, 5735−5739.

(15) Haines, D. C.; Tomchick, D. R.; Machius, M.; Peterson, J. A. Pivotal role of water in the mechanism of P450BM-3. *Biochemistry* **2001**, *40*, 13456−13465.

(16) Sevrioukova, I. F.; Li, H.; Zhang, H.; Peterson, J. A.; Poulos, T. L. Structure of a cytochrome P450-redox partner electron-transfer complex. *Proc. Natl. Acad. Sci. U.S.A.* **1999**, *96*, 1863−1868.

(17) Kumar, S.; Halpert, J. R. Use of directed evolution of mammalian cytochromes P450 for investigating the molecular basis of enzyme function and generating novel biocatalysts. *Biochem. Biophys. Res. Commun.* **2005**, *338*, 456−464.

(18) Straathof, A. J.; Panke, S.; Schmid, A. The production of fine chemicals by biotransformations. *Curr. Opin. Biotechnol.* **2002**, *13*, 548−556.

(19) Wen, Z.; Baudry, J.; Berenbaum, M. R.; Schuler, M. A. Ile115Leu mutation in the SRS1 region of an insect cytochrome P450 (CYP6B1) compromises substrate turnover via changes in a predicted product release channel. *Protein Eng. Des. Sel.* **2005**, *18*, 191−199.

(20) Yeom, H.; Sligar, S. G. Oxygen activation by cytochrome P450BM-3: effects of mutating an active site acidic residue. *Arch. Biochem. Biophys.* **1997**, *337*, 209−216.

(21) Guenther, M. G.; Witmer, M. R.; Burke, J. R. Cytosolic phospholipase A2 shows burst kinetics consistent with the slow, reversible formation of a dead-end complex. *Arch. Biochem. Biophys.* **2002**, *398*, 101−108.

(22) Farinas, E.; Schwaneberg, U.; Glieder, A.; Arnold, F. H. Directed evolution of a Cytochrome P450 Monooxygenase for Alkane Oxidation. *Adv. Synth. Catal.* **2001**, *343*, 601−606.

(23) Bauer, S.; Shiloach, J. Maximal exponential growth rate and yield of E. coli obtainable in a bench-scale fermentor. *Biotechnol. Bioeng.* **1974**, *16*, 933−941.

(24) Lussenburg, B. M. A.; Keizers, P. H. J.; de Graaf, C.; Hidestrand, M.; Ingelman-Sundberg, M.; Vermeulen, N. P. E.; Commandeur, J. N. M. The role of phenylalanine 483 in cytochrome P450 2D6 is strongly substrate dependent. *Biochem. Pharmacol.* **2005**, *70*, 1253−1261.

(25) MOE, Chemical Computing Group Inc.: Montreal, Quebec, Canada.

(26) Jones, G.; Willett, P.; Glen, R. C.; Leach, A. R.; Taylor, R. Development and validation of a genetic algorithm for flexible docking. *J. Mol. Biol.* **1997**, *267*, 727−748.

(27) Christen, M.; Hunenberger, P. H.; Bakowies, D.; Baron, R.; Burgi, R.; Geerke, D. P.; Heinz, T. N.; Kastenholz, M. A.; Krautler, V.; Oostenbrink, C.; Peter, C.; Trzesniak, D.; van Gunsteren, W. F. The GROMOS software for bioMol. Simul.: GROMOS05. *J. Comput. Chem.* **2005**, *26*, 1719−1751.

(28) Berendsen, H. J. C.; van der Spoel, D.; van Drunen, R. GROMACS: A message-passing parallel molecular dynamics implementation. *Comp. Phys. Commun.* **1995**, *91*, 43−56.

(29) Lindahl, E.; Hess, B.; van der Spoel, D. GROMACS 3.0: A package for Molecular Simulation and trajectory analysis. *J. Mol. Mod.* **2001**, *7*, 306−317.

(30) Schuler, L. D.; Daura, X.; van Gunsteren, W. F. An improved GROMOS96 force field for aliphatic hydrocarbons in the condensed phase. *J. Comput. Chem.* **2001**, *22*, 1205−1218.

(31) van Gunsteren, W. F.; Billeter, S. R.; Eising, A. A.; Hunenberger, P. H.; Kruger, P.; Mark, A. E.; Scott, W. R. P.; Tironi, I. G. *Biomolecular Simulation: The GROMOS96 manual and user guide*; Vdf Hochschulverlag AG an der ETH Zurich: Zurich, 1996.

(32) Keizers, P. H. J.; de Graaf, C.; de Kanter, F. J.; Oostenbrink, C.; Feenstra, K. A.; Commandeur, J. N. M.; Vermeulen, N. P. E. Metabolic regio- and stereoselectivity of cytochrome P450 2D6 towards 3,4-methylenedioxy-*N*-alkylamphetamines: in silico predictions and experimental validation. *J. Med. Chem.* **2005**, *48*, 6117−6127.

(33) Tew, D. G. Inhibition of cytochrome P450 reductase by the diphenyliodonium cation. Kinetic analysis and covalent modifications. *Biochemistry* **1993**, *32*, *10209*−10215.

(34) Note: the equation described by Noble et al. contains a typographical error; one of the parentheses is misplaced.

JM0609061